# INFLUENCE OF IONIC ENVIRONMENT AND pH ON THE ELECTROKINETIC PROPERTIES OF BALL CLAYS

Carmen Galassi[1], Anna Luisa Costa[1] and Paolo Pozzi[2]

[1] IRTEC-CNR, Via Granarolo 64, I-48018 Faenza (RA), Italy
[2] Dip. di Chimica, Università di Modena e Reggio Emilia, Via Campi 183, I-41100 Modena, Italy

**Abstract**—Three ball clays (SP from England, TSMA from France and UK from the Ukraine) were characterized for their dry and wet colloidal properties. On the basis of X-ray diffraction and chemical analyses the clays were classified as kaolinite-rich clay, smectitic kaolinite-rich clay and illitic kaolinite-rich clay. The $\zeta$ (zeta) potential at the clay-water interface as a function of pH, in three different electrolytes, was investigated using an electroacoustic technique. Starting from measurements of dynamic mobility, the calculated $\zeta$ potential was found to be almost constant as a function of pH for the TSMA and UK clays, while it increased from $-20$ to $-60$ for the SP clay, when potassium nitrate was used as an electrolyte. The behavior of the three clays in calcium and magnesium nitrate was slightly different: SP showed a smaller increase in $\zeta$ potential, while a small deviation from the constant behavior of the UK clay was found. The results are explained in terms of the surrounding-ion atmosphere in light of the chemical-physical properties measured. Our results may well be of use to those involved in ceramic processing.

**Key Words**—Cation Exchange Capacity, Clay Minerals, Electroacoustic, Electrolytes, Structural Properties, Surface Charge, $\zeta$ Potential.

## INTRODUCTION

In industrial processing, ceramic raw materials are frequently handled as suspensions. They are milled in water and the suspensions are stored and transported, spray dried into granules, partially dried for working in the plastic state or consolidated directly through casting techniques. Ceramic raw materials show a broad range of particle sizes, from tens of microns to the colloidal range. Clays play a critical role in the control of the overall performance of the suspensions. Besides the concentration of the solids, the physics of the particles (density, size distribution, specific surface area, shape), the flow properties of the suspensions and their compaction behavior are strongly influenced by reactions at the solid-liquid interface and interparticle interactions which are mostly electrostatic and govern the aggregation of the dispersed phase. Improved performance in the cold consolidation stage, storage of slurry without formation of thick sediments, and efficient transportation through pipes are only a few examples of industrial processing improvements arising from the modulation of the suspension state from well dispersed to weakly or strongly flocculated. Moreover, there is a great need to develop techniques for the investigation of the interactions of the raw materials, especially those in the colloidal range, with the surrounding medium. In industrial practice, the dispersing medium is never distilled water. The raw materials (that are commonly employed as received, without purification), and the natural or recycled water used to disperse the clay contribute ions to the system.

In this study an electroacoustic technique was used to characterize the aqueous clay suspensions and to determine $\zeta$ potential values as a function of suspension parameters like pH and conductivity at values of clay concentration near those of typical industrial application. The $\zeta$ potential variation as a function of pH was tested for three different ball clays in three different electrolyte solutions: $KNO_3$, $Ca(NO_3)_2$ and $Mg(NO_3)_2$ and the results were interpreted on the basis of the surface reactivity, taking into account the mineralogical, physical and chemical properties of these clays. The three electrolytes were chosen because these cations are commonly present in industrial water supplies and because a study of the influence of the ions present in water from an electrokinetic point of view can increase understanding of the performance of clay-water dispersions. The clays were used as received from the suppliers to investigate their contribution to the dispersing behavior of the ceramic body.

## EXPERIMENTAL

### Materials

Three commercial ball clays, Standard Porcelain (ECC International) from England (referred to below as SP), TSMA (DAMREC) from France (referred to below as TSMA) and UK1 (COMBINAT CHASOV YAR) from Ukraine (referred to below as UK), commonly used in the formulation of traditional ceramic bodies, were analyzed. According to the prevailing clay mineral in their composition they can be classified as kaolinite-rich clay (SP), smectitic kaolinite-rich clay (TSMA) and illitic kaolinite-rich clay (UK), respectively.

Table 1. Mineralogical composition of clays (%).

| Mineral | SP clay | TSMA clay | UK clay |
|---|---|---|---|
| Quartz | 8 | 31 | 34 |
| Kaolinite | 80 | 43 | 37 |
| Illite | 9 | 6 | 23 |
| Smectite | 0 | 14 | 0 |
| Other clay minerals | 3 | 6 | 6 |

## Methods

The mineralogy was determined on bulk powder samples packed into an end-loading powder holder by X-ray diffraction (XRD, Rigaku 2003, Japan) using CuKα radiation and a scanning speed of 1°2θ/min. Quantitative mineralogical composition was determined on the basis of XRD and chemical data according to the method used by Fabbri *et al.* (1986). The specific surface area (SSA) was determined by the nitrogen adsorption method, using a multi-point nitrogen adsorption Micromeritics Gemini 2360 (USA) instrument (the samples were outgassed for 240 min at 200°C, before SSA measurements). The particle size distribution was determined using a Fritsch Laser Particle Sizer Analysette 22, and the particle morphology was ascertained with a scanning electron microscope (SEM), Leica Cambridge Stereoscan 360.

The chemical composition was determined by inductively coupled plasma-optical emission spectrometry (ICP-OES, Varian Liberty 200, Australia). The analytical solutions were prepared by alkaline fusion with $LiBO_2$ and by dissolving the final samples in $HNO_3$ at 10 wt.%, using the method suggested by Jeffery and Hutchison (1981). Cation exchange capacities of the clay samples were determined using a methylene blue method, according to the procedure suggested by Hang and Brindley (1970). The exchangeable alkali ($Na^+$, $K^+$) and alkaline-earth ($Ca^{2+}$, $Mg^{2+}$) cations were determined by ICP-OES by suspending 1 g of clay in 100 mL of LiCl (1 M) solution for 24 h at 20°C. The electrokinetic characterization was obtained with the Acoustosizer (AZR, Colloidal Dynamics, Australia), through the determination of the dynamic mobility on clay-water dispersions. The samples were prepared at an electrolyte strength of 10 mM in three different electrolyte solutions: $KNO_3$ (Merck), $Ca(NO_3)_2$ (Carlo Erba) and $Mg(NO_3)_2$ (Carlo Erba) at 0.10 volume fraction. The powders were ball-milled in the electrolyte solution for 1 h with 1:1 by weight alumina grinding media without any preliminary chemical treatment. Then the slurries were placed in the Acoustosizer, thermally equilibrated at 25°C, and the pH was allowed to stabilize around its natural value for a few minutes. The automatic titration software was used to measure ζ potential as a function of pH between two fixed points; in the case of clay SP and TSMA the starting point was the unadjusted pH
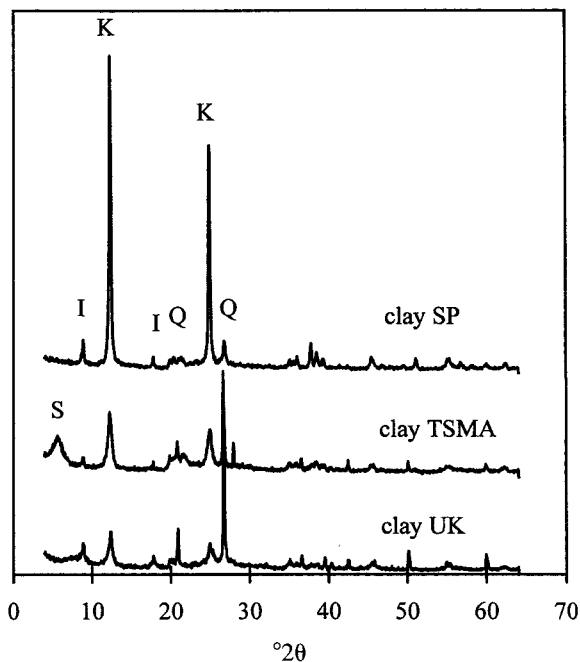


Figure 1. XRD patterns of the SP, TSMA and UK clays: K, S, I and Q identify the main peaks of kaolinite, smectite, illite and quartz, respectively.

(around 4) and the final pH was 10–11; in the case of clay UK, the pH (~7.5) of the as-prepared suspension was adjusted to a basic pH (~10) and decreased during the analysis from ~10 to a final pH of 4. $HNO_3$ (4 M) and KOH (1 M) were used to adjust the pH.

## RESULTS AND DISCUSSION

### Chemical-mineralogical-morphological characterization of the clays

The mineralogical composition of the clays is reported in Table 1 and Figure 1. Quartz is present in large amounts in the TSMA and UK clays, and kaolinite is the predominant clay mineral in all three clays. The mean diameter is reported in Table 2 as are the specific surface areas. The mean diameter values, measured using the laser technique, result from the contribution of particles with very different sizes, all in-

Table 2. Mean diameter, specific surface area, density of clays.

| Material | Mean diameter[1] $D_{50}$ (μm) | Specific surface area[2] ($m^2/g$) | Density ($g/cm^3$) |
|---|---|---|---|
| SP clay | 4.72 | 13.91 | 2.48 |
| TSMA clay | 5.51 | 36.98 | 2.49 |
| UK clay | 4.03 | 27.40 | 2.57 |

[1] Determined with a Fritsch Laser Particle Sizer Analysette 22.

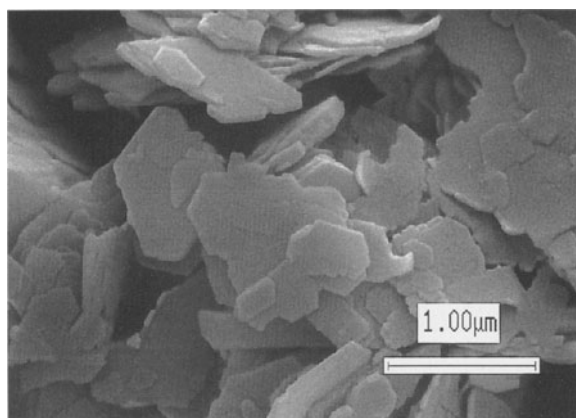[2] Determined by the nitrogen adsorption method.

Figure 2. SEM morphology of SP clay powder.

Table 4. Total and specific CEC (meq/100 g) of clay.

| Clay | Total | $Na^+$ | $K^+$ | $Ca^{2+}$ | $Mg^{2+}$ |
|------|-------|--------|-------|-----------|-----------|
| SP | 2.14 | 0.76 | 0.56 | 0.38 | 0.27 |
| TSMA | 6.54 | 0.26 | 0.81 | 4.23 | 1.17 |
| UK | 5.25 | 1.54 | 0.27 | 2.60 | 0.83 |

cluded in the measuring range of the instrument. Quartz particles have dimensions which are typically >10 μm. Consequently the quartz fraction does not significantly influence the colloidal properties of the suspensions nor the data collected from electrokinetic measurements. The SEM morphology of the clays (SEM morphology of SP clay is reported in Figure 2 as an example) was determined in order to calculate the aspect ratios. In Tables 3 and 4 the chemical composition and the CECs of clays are reported. Comparing the values of chemical composition and CEC, it is possible to estimate the ionic species responsible for surface charge compensation in the solution systems considered. The TSMA clay contains mostly $Ca^{2+}$ and $Mg^{2+}$ cations, most of them exchangeable (Table 3, CaO + MgO content (%): TSMA 1.53, UK 0.97, SP 0.83; Table 4, CEC of $Ca^{2+}$ + $Mg^{2+}$ (meq/100 g): TSMA 5.4, UK 3.43, SP 0.65) while the UK clay contains more cations, most of them $K^+$ which are not exchangeable (Table 3, $K_2O$ content (%): UK 1.93, SP 0.77, TSMA 0.56; Table 4, CEC of $K^+$ (meq/100 g): UK 0.27, SP 0.56, TSMA 0.81). The SP clay has the lowest CEC and a minor quantity of cations adsorbed onto the surface.

*Electrokinetic characterization*

*Clay-water interactions.* The three ball clays used were characterized and classified on the basis of their prevailing composition as kaolinite-rich clay, smectitic kaolinite-rich clay and illitic kaolinite-rich clay.

In concentrated ceramic suspensions, the interparticle interactions dominate and the degree of colloidal stability depends on whether the attractive or repulsive force prevails. The repulsive potential energy between charged particles supports colloidal stability and depends on the surface potential $\psi_0$. In most cases the only electrical potential that can be measured is the $\zeta$ potential, defined as the electrical potential at the plane of the transition between zero and bulk fluidity (slipping plane), (Lyklema, 1987). This potential actually controls particle interactions and it is justifiable to use it instead of $\psi_0$ in the equations for electrostatic repulsion. Furthermore, the determination of $\zeta$ potential that results from surface charge compensation by ionic species adsorbed into the region closest to the solid surface is fundamental in detecting the nature of the surface and the specifically adsorbed species (Lyklema, 1987; Pugh and Bergström, 1994).

Several monographs (Grim, 1968; Grimshaw, 1971; Worral, 1975) describe the mineralogy of clays while clay colloid behavior is approached from a double layer point of view in Van Olphen (1977), Dixon *et al.* (1977), Greenland and Hayes (1978), Barrow (1987) and Lyklema (1995). Lyklema (1995), in discussing the double layer properties of clay minerals, emphasizes the difficulty in interpreting electrokinetic properties due to the heterogeneity of the clay mineral particle shape and charge distribution. The charges in the basal faces are independent of pH and salt concentration (Constant Basal Surface Charge, CBSC model), while the Al-oxy/hydroxy groups at the edge sites show typical pH and ionic species-dependent charge behavior.

Sondi *et al.* (1996, 1997), in their work on electrokinetic potentials of pure clay minerals, used oxides as models for clay surfaces and concluded that the clay particle edge sites, well represented by a $\gamma$-$Al_2O_3$ surface model, are the most active clay mineral sites in interactions with an aqueous medium and its ionic components.

Table 3. Chemical composition expressed as wt. % of equivalent oxide of clays.

| Clay | $SiO_2$ | $Al_2O_3$ | CaO | MgO | $Na_2O$ | $K_2O$ | $Fe_2O_3$ | $TiO_2$ | LOI[1] |
|------|---------|-----------|-----|-----|---------|--------|-----------|---------|------|
| SP | 49.2 | 35.2 | 0.48 | 0.35 | 0.31 | 0.77 | 0.70 | 0.05 | 11.8 |
| TSMA | 61.0 | 22.1 | 0.63 | 0.90 | 0.11 | 0.56 | 1.74 | 0.71 | 8.5 |
| UK | 62.7 | 22.5 | 0.37 | 0.60 | 0.40 | 1.93 | 1.15 | 1.28 | 6.7 |

[1] Loss on ignition.

Table 5. Electrokinetic and electrochemical measurements made with the Acoustosizer.[1]

| Clay | Electrolyte | Natural pH | Conductivity (S/m) | $\zeta$ (mV) | $D_{50}$ ($\mu$m) |
|------|-------------|-----------|---------------------|--------------|-------------------|
| SP   | $KNO_3$     | 4.20      | 0.12                | $-21.8$      | 0.63              |
| TSMA | $KNO_3$     | 4.00      | 0.20                | $-10.2$      | 0.67              |
| UK   | $KNO_3$     | 7.70      | 0.12                | $-24.3$      | 0.89              |
| SP   | $Ca(NO_3)_2$| 4.00      | 0.20                | $-10.2$      | 0.35              |
| TSMA | $Ca(NO_3)_2$| 4.00      | 0.29                | $-10.4$      | 0.58              |
| UK   | $Ca(NO_3)_2$| 7.20      | 0.21                | $-18.8$      | 0.85              |
| SP   | $Mg(NO_3)_2$| 4.50      | 0.19                | $-10.0$      | 0.40              |
| TSMA | $Mg(NO_3)_2$| 3.90      | 0.28                | $-10.7$      | 0.55              |
| UK   | $Mg(NO_3)_2$| 7.60      | 0.21                | $-18.1$      | 0.71              |

[1] Suspensions at 10 vol. % solids.

It can be said that in clay water suspensions, $\zeta$ potential is governed by the absolute charge developed on the basal surfaces and by the residual potential at the slipping plane around the edges. The cloud of ions interacting with clay edges is formed by species specifically adsorbed on the surface as protons, bi- and trivalent cations leached from the layer structure, or humic acids always present in natural water, and by alkali ions exhibiting only Coulomb interactions. Hofmeister (Grim, 1968) determined the relative degree of interaction between various cations and the clay particle surfaces ($H^+>Al^{3+}>Ca^{2+}>Mg^{2+}>NH_4^+>K^+>Na^+>Li^+$). The first cations have the greater charge and the lower hydration shell so they will reside closest to the surface. For this reason they are called coagulating ions and their high negative surface charge compensation effect and narrow hydration shell make a close approach between clay particles possible. Otherwise, the alkaline cations do not influence the surface charge directly and reside at fairly large distances from it. For this reason these alkaline cations are called deflocculating ions.

*$\zeta$ potential determination*

The $\zeta$ potential and particle size data are calculated from dynamic mobility values obtained from measurements of the ESA (electrokinetic sonic amplitude) signal of the charged particles in non-dilute suspensions (powder concentration up to 25% by volume). In order to make this calculation from dynamic mobility data, the particles are assumed to be spherical with thin double layers (O'Brien and Rowlands, 1995). This assumption seems to be incorrect in the case of clay minerals which generally have plate-shaped particles. Nevertheless Loewemberg and O'Brien (1992) demonstrated that the same formulae used for spherical particles can be used for determining the $\zeta$ potential and equivalent size of platey particles with thin double layers and low surface conductance. In fact, the equivalent sphere radius of a disc-shaped particle with an aspect ratio $r$ and disc radius $r_d$ is approximately $r_s \approx r_d\sqrt{r}$ provided that $0.1 \leq r \leq 0.3$. Futhermore, although clay minerals show significant surface conduc-
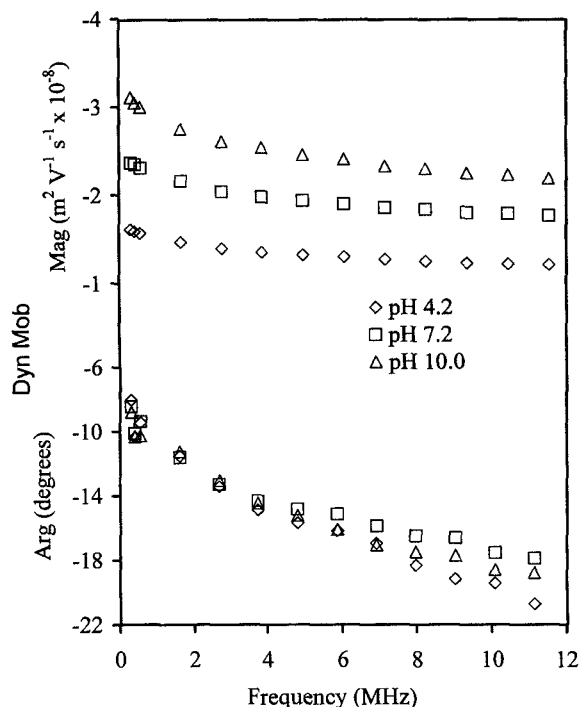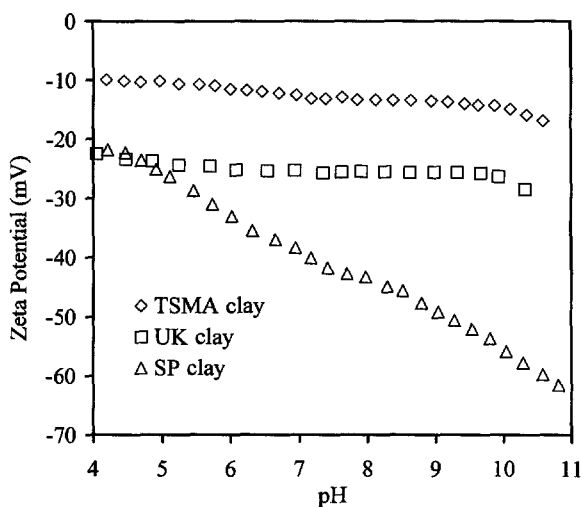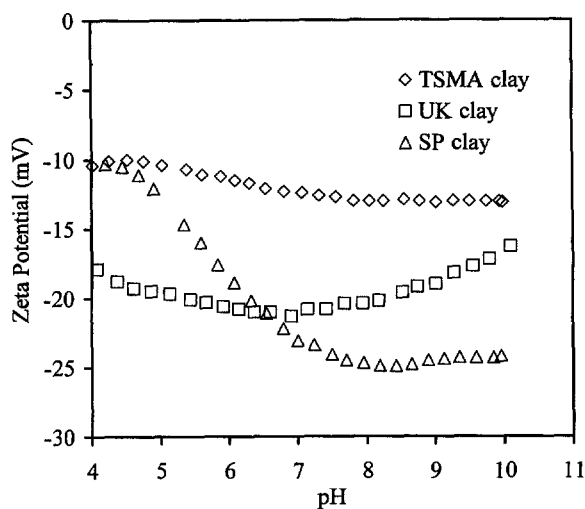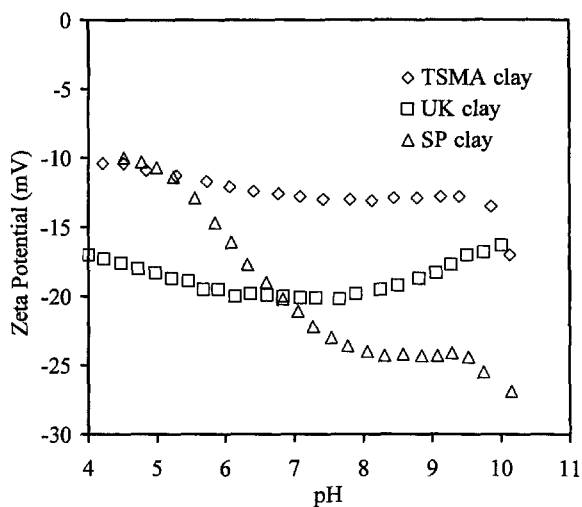


Figure 3.  Magnitude and argument of dynamic mobility *vs.* frequency (SP clay in potassium nitrate).

tance, as Rasmusson *et al.* and O'Brien and Rowlands showed in their papers on dynamic mobility of sodium bentonite and kaolinite (Rasmusson *et al.*, 1997; O'Brien and Rowlands, 1995), the assumption of low surface conduction can be made. This assumption is justified in this study, because we checked all measurements of dynamic mobility magnitude and phase as a function of frequency and found that the trend is that expected from the theoretical formula applied in the AZR software (O'Brien and Rowlands, 1995). In all cases we also tried to lower the pH to 2 to check if an isoelectric point (iep, the solution condition at which $\zeta$ potential is zero) existed, but it was never reached, as was predicted by Lyklema (1995). In fact for all clay minerals tested, the $\zeta$ potential remains negative over the entire accessible pH range, decreasing in magnitude with decreasing pH.

Some electrokinetic and electrochemical data, referring to measurements made with the Acoustosizer, before adjusting the pH of the suspensions (natural pH), are summarized in Table 5. The natural pH, the suspension conductivity, the $\zeta$ potential and the mean diameter of the particles, calculated by the Acoustosizer software, are shown. The natural pH refers to the pH of the suspensions as prepared, and gives important information about the surface chemical reactivity. In Figure 3 the dynamic mobility argument and magnitude of SP clay, in $KNO_3$ solution, is reported as a function of the frequencies applied. These curves were

Figure 4.  ζ potential *vs.* pH in potassium nitrate.



Figure 6.  ζ potential *vs.* pH in magnesium nitrate.

also calculated and evaluated for the TSMA and UK clays, in every electrolyte, to check possible anomalous surface conductance effects. The dynamic mobility argument and magnitude as a function of frequency decrease monotonically with frequency, as expected from O'Brien and Rowlands' theoretical formula (1995). This confirms that, at this ionic strength, the anomalous surface conductance of clay minerals in suspensions has no effect, and we can use the AZR software to extract real values of ζ potential and particle size for these systems. The mean particle diameters, measured using the Acoustosizer (Table 5), were compared to the particle diameters determined from SEM photographs (Figure 2), although the sample preparation procedure was substantially different. The results of this comparison gave the same order of mag-

nitude, ~1 μm, which differed, as expected, from the mean particle size determined by the laser technique (Table 2). As already discussed, this discrepancy can be attributed to the contribution of quartz particles, which is not taken into account in the determination through SEM images or electrokinetic analysis. In Figures 4, 5 and 6, the ζ potential curves as a function of pH for the SP, TSMA and UK clay suspensions prepared in $KNO_3$, $Ca(NO_3)_2$ and $Mg(NO_3)_2$ solutions, respectively, are shown. In Figure 7 the conductivity as a function of pH for UK clay suspensions prepared in $KNO_3$, $Ca(NO_3)_2$ and $Mg(NO_3)_2$ solutions is reported.

To understand the surface charge properties of clay minerals, several studies have considered the isolated contribution of $SiO_2$ and Al-oxy-hydroxy surfaces (Van Olphen, 1977; Lyklema, 1995; Rowlands and O'Brien, 1995; Sondi *et al.*, 1997; Schroth and
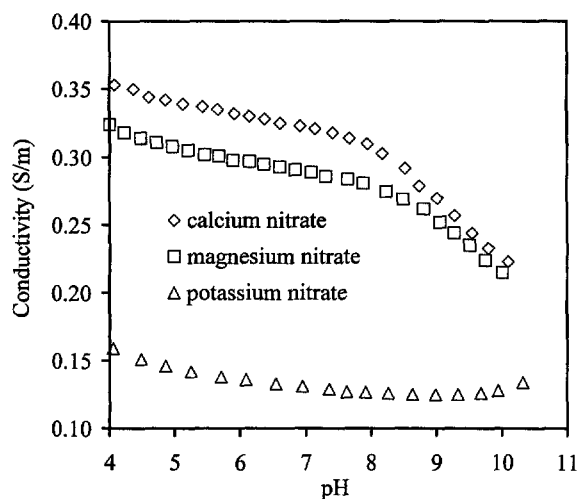


Figure 5.  ζ potential *vs.* pH in calcium nitrate.



Figure 7.  Conductivity *vs.* pH (UK clay).

Sposito, 1997; Tarì *et al.*, 1999). In particular, Sondi *et al.* (1997) compared the ζ potential of silica, gibbsite [γ-Al(OH)₃] and aluminum oxide (γ-Al₂O₃) as a function of pH to simulate the surface charge properties of the basal silica plane, of the basal aluminum oxide plane, and of the 'aluminol' edge sites, respectively. Based on this approach, the mineralogical, chemical and electrokinetic data in this paper can be explained. As expected, the ζ potential remains negative for all samples in the whole pH region investigated (Figures 4–6). Taking into account that the pH of the isoelectric point (pHiep) for $SiO_2$ is <2, for gibbsite is ~5, and for γ-$Al_2O_3$ is ~9.5, it can be concluded that the ζ potential is mainly influenced by basal siloxane surface charge rather than by that of aluminol amphoteric surface. The absolute value of negative charge will depend on Si(IV)/Al(III) substitution as well as on charged species chemically adsorbed onto the surfaces. Comparing the ζ potential values at natural pH (Table 5), it can be seen that, in $KNO_3$, the SP and UK clays show the higher negative values of ζ potential (~−20 mV) while the TSMA clay shows a ζ potential of −10 mV. The difference between the UK and TSMA clays can be explained by considering the different ion atmosphere surrounding these surfaces. Taking into account the ion exchange capacity data (Table 4, exchanged $Mg^{2+}$ + $Ca^{2+}$ content (meq/100 g): TSMA 5.4, UK 3.43) and the conductivity data (Table 5, conductivity (S/m): TSMA 0.20, UK 0.12), we can conclude that TSMA clay particles are surrounded by a greater number of bivalent cations that compensate the surface charge. In contrast, the UK and SP clays are surrounded by a greater number of monovalent ions (Table 4, exchanged $Na^+$ + $K^+$ content (meq/100 g): UK 1.81, SP 1.32, TSMA 1.07). In $Ca^{2+}$ and $Mg^{2+}$ solutions, the monovalent ions can easily be replaced by bivalent cations as the Hofmeister's series suggests (Grim, 1968). For this reason the SP and UK clays show lower ζ potentials in $Ca(NO_3)_2$ and $Mg(NO_3)_2$ than in $KNO_3$.

In Figure 4 the ζ potential trends *vs.* pH for SP, TSMA and UK clays in $KNO_3$ are compared. It can be seen that only SP clay shows a pH dependency of ζ potential varying from ~−20 mV (pH 4) to ~−60 mV (pH 11). The other two clays show ζ potential curves that are reasonably constant *vs.* pH. These trends can be explained on the basis of the clays' mineralogy. The SP clay contains 80% kaolinite, a 1:1 layer mineral, while the TSMA and UK clays contain 20% and 23% 2:1 layer minerals, respectively (Table 1). Considering that in the pH range investigated, $SiO_2$ shows a negative value of ζ potential, quite constant *vs.* pH (from ~−40 to ~−50 mV) (Sondi, 1997; Tarì *et al.*, 1999), the abrupt decrease in ζ potential with increasing pH, for the SP sample, is essentially due to deprotonation of hydrated alumina surfaces. In the case of the TSMA and UK clays, the smaller total

content of clay minerals, the reduced amount of alumina compared to silica and the larger amount of bivalent cations adsorbed on the surface strongly reduce the pH-charge dependency. The SP ζ potential trend *vs.* pH in $Ca(NO_3)_2$ and $Mg(NO_3)_2$ is quite different in comparison with that in $KNO_3$ (Figures 5, 6). The absolute value of the ζ potential increases from the natural pH to pH 7 (from ~−10 to ~−25) and remains constant in the higher pH range. The ζ potential increases during the neutralization of alumina positive sites up to pH 8. This can be explained by the adsorption of $Ca^{2+}$ and $Mg^{2+}$ ions from electrolytes, which counterbalances the increasing negative charge due to hydrated alumina deprotonation. The TSMA clay shows the same behavior in the three electrolytes, with ζ potential remaining at ~−10 mV in the whole pH range examined. In this case the humic acids and the bivalent cations already present on the clay surface (see data in Tables 3 and 4) screen the surface and make it independent of pH. The UK ζ potential curves in $Ca(NO_3)_2$ and $Mg(NO_3)_2$ are slightly different than in $KNO_3$. The ζ potential remains nearly constant in $KNO_3$, while in $Mg(NO_3)_2$ and $Ca(NO_3)_2$ it shows a maximum at ~pH 7, and then begins to decrease (from ~−21 mV at pH 7 to ~−16 mV at pH 10 in both cases). These data cannot be justified on the basis of the UK clay conductivity data reported in Figure 7. In fact, conductivity increases (from 0.22 S/m to 0.32 S/m in $Ca(NO_3)_2$) in the same basic pH range where ζ potential increases as well, changing pH from 10 to 8. This can be explained by considering that the UK negative surface is screened by a larger amount of cations (most of them $K^+$, which are not exchangeable) in comparison with SP and TSMA clays. For this reason, the added protons have practically no effect on the surface charge nor on the conductivity or ζ potential values in $KNO_3$ solution unlike $Ca(NO_3)_2$ and $Mg(NO_3)_2$ solutions. In $Ca(NO_3)_2$ and $Mg(NO_3)_2$ solution the protons replaced $Mg^{2+}$ and $Ca^{2+}$ cations, adsorbed onto the surface in the basic region, reducing the screening effect of bivalent cations near the surface. Consequently the absolute value of ζ potential and the conductivity in the dispersing phase increase. These experimental results prove the different colloidal behaviors of the three natural clays examined. Two of them exhibit a substantially similar trend of the ζ potential as a function of pH in the three electrolytes; the TMSA showing constant values, always ranging around −10 mV and the UK, with slight variations, in the −15 mV to −25 mV range. The performance of SP is very different, the ζ potential depending strongly on pH and reaching values as high as −60 mV in $KNO_3$.

## CONCLUSIONS

The colloidal properties of the water-based suspensions of three natural ball clays classified as kaolinite-

rich clay, smectitic kaolinite-rich clay and illitic kaolinite-rich clay studied by determination of electrokinetic potential at the solid-liquid interface, were correlated with physical, chemical and mineralogical parameters. The electroacoustic technique provided information that can improve the formulation of the ceramic bodies, despite the complexity of the surface reactivity of the clay-based systems. Knowledge of the pH or cation type dependence of the surface potential contributes to the improvement of the formulation, or allows the explanation of the phenomenological performance of the slurries that could be investigated through rheological characterization. For example, the colloidal stability of SP clay-based bodies depends on pH and on variation of electrolytes in the industrial water, whereas the TSMA and UK-based bodies are less sensitive to these parameters.

## ACKNOWLEDGEMENTS

## REFERENCES

Barrow, N.J. (1987) *Reactions with Variable Charge Sols.* M. Nijhoff, Dordrecht, The Netherlands.

Dixon, J.B., Weed, S.B. and Rich, C.I., editors (1977) *Minerals in Soil Environments.* Soil Science Society of America, Madison, Wisconsin, 948 pp.

Fabbri, B., Fiori, C., Krajewski, A., Valmori, R. and Tenaglia, A. (1986) Comparison between traditional mineralogical and computerized rational analysis of ceramic raw materials. *Journal de Physique,* **47,** 57–62.

Greenland, D.J. and Hayes, M.H.B., editors (1978) *The Chemistry of Soil Constituents.* Wiley, New York, 508 pp.

Grim, R. E. (1968) *Clay Mineralogy,* 2nd edition. McGraw Hill, New York.

Grimshaw, R.W. (1971) *The Chemistry and Physics of Clays,* 4th edition. Wiley Interscience, New York, 256 pp.

Hang, P.T. and Brindley, G.W. (1970) Methylene blue adsorption by clay minerals. Determination of surface areas and cation exchange capacities (clay-organic study XVIII). *Clays and Clay Minerals,* **18,** 203–212.

Jeffery, P.G. and Hutchison, D. (1981) *Chemical Methods of Rock Analysis.* Pergamon Press, Oxford, UK.

Loewemberg, M. and O'Brien, R.W. (1992) The dynamic mobility of nonspherical particles. *Journal of Colloid and Interface Science,* **150,** 158–168.

Lyklema, J. (1987) Structure of the solid/liquid interface and the electrical double layer. Pp. 63–90 in: *Solid/Liquid Dispersions* (Th. F. Tadros, editor). Academic Press, London, 331 pp.

Lyklema, J. (1995) *Fundamentals of Interface and Colloid Science Volume II: Solid-Liquid Interfaces.* Academic Press, London.

O'Brien, R.W. and Rowlands, W.N. (1995) Electroacoustic determination of particle size and zeta potential. *Journal of Colloid and Interface Science,* **173,** 406–418.

Pugh, R.J. and Bergström, L., editors (1994) *Surface and Colloid Chemistry in Advanced Ceramics Processing.* Surfactant Science Series, Vol. 51, Marcel Dekker, New York, 363 pp.

Rasmusson, M., Rowlands, W.N., O'Brien, R.W. and Hunter, R.J. (1997) The dynamic mobility and dielectric response of sodium bentonite. *Journal of Colloid and Interface Science,* **189,** 92–100.

Rowlands, W.N. and O'Brien, R.W. (1995) The dynamic mobility and dielectric response of kaolinite particles. *Journal of Colloid and Interface Science,* **175,** 190–200.

Schroth, B.K. and Sposito, G. (1997) Surface charge properties of kaolinite. *Clays and Clay Minerals,* **45,** 85–91.

Sondi, I. and Pravdić, V. (1996) Electrokinetics of natural and mechanically modified ripidolite and beidellite clays. *Journal of Colloid and Interface Science,* **181,** 463–469.

Sondi, I., Bišćan, J. and Pravdić, V. (1996) Electrokinetics of pure clay minerals revisited. *Journal of Colloid and Interface Science,* **178,** 514–522.

Sondi, I., Milat, O. and Pravdić, V. (1997) Electrokinetic potential of clay surfaces modified by polymers. *Journal of Colloid and Interface Science,* **189,** 66–73.

Tarì, G., Bobos, J., Gomes, C.S.F. and Ferreira, J.M.F. (1999) Modification of surface charge properties during kaolinite to halloysite-7Å transformation. *Journal of Colloid and Interface Science,* **210,** 360–366.

Van Olphen, H. (1977) *An Introduction to Clay Colloid Chemistry for Clay Technologists, Geologists and Soil Scientists,* 2nd edition. Wiley, New York, 318 pp.

Worral, W.E. (1975) *Clays and Ceramic Raw Materials.* Applied Science Publishers, Glasgow, 203 pp.